

Screening for T-DNA insertion lines

We used the T-DNA insertion-line screening system organized at the Kazusa DNA Research Institute. The principles of the screening method were as described²⁵. Gene-specific primers were 5'-ATATGCGATAGCGACTCTCGTACAA-3' and 5'-AAC-CAAAATGCATATCAATCAGCAG-3'. T-DNA (pPCVEn4HPT)²⁶ specific primers were 5'-ATAACGCTGCGGACATCTAC-3' and 5'-ATCTAGGCTTTGATAGTCAC-3'. We used four combinations of primer sets, each consisting of a gene specific primer and a T-DNA-specific primer. The position of the T-DNA insert was determined by sequencing the PCR products carrying the T-DNA-genome junctions.

Yeast experiments

The entire coding region of the CRE1a cDNA was PCR-amplified and cloned into the yeast expression vector p415CYC²⁷ under the CYC1 promoter at the *Sma*I site, generating p415CYC-CRE1. We used the QuickChange site-directed mutagenesis kit (Stratagene) to generate p415CYC-CRE1(G467D), p415CYC-CRE1(H459Q) and p415CYC-CRE1(D973N). After sequence confirmation, plasmids were introduced into *sln1Δ* (strain TM182¹⁰) or *ypd1Δ* (strain SW100¹⁷). Suspensions of transformants were spotted (about 800 cells per spot) onto drop-out media with 10 μM plant hormones as indicated in Fig. 4, with either 2% glucose or 2% galactose.

Received 16 October; accepted 8 December 2000.

1. Skoog, F. & Miller, C. O. Chemical regulation of growth and organ formation in plant tissues cultured in vitro. *Symp. Soc. Exp. Biol.* **11**, 118–131 (1957).
2. Mok, M. C. in *Cytokinins* (eds Mok, D. W. S. & Mok, M. C.) 155–166 (CRC, Boca Raton, 1994).
3. Kakimoto, T. CK11, a histidine kinase homolog implicated in cytokinin signal transduction. *Science* **274**, 982–985 (1996).
4. Sakakibara, H. *et al.* A response-regulator homologue possibly involved in nitrogen signal transduction mediated by cytokinin in maize. *Plant J.* **14**, 337–344 (1998).
5. Brandstatter, I. & Kieber, J. J. Two genes with similarity to bacterial response regulators are rapidly and specifically induced by cytokinin in *Arabidopsis*. *Plant Cell* **10**, 1009–1019 (1998).
6. Mizuno, T. His-Asp phosphotransfer signal transduction. *J. Biochem.* **123**, 555–563 (1998).
7. D'Agostino, I. B. & Kieber, J. J. Phosphorelay signal transduction: the emerging family of plant response regulators. *Trends Biochem. Sci.* **24**, 452–456 (1999).
8. Chang, C., Kwok, S. F., Bleecker, A. B. & Meyerowitz, E. M. *Arabidopsis* ethylene-response gene *ETR1*: similarity of product to two-component regulators. *Science* **262**, 539–544 (1993).
9. Schaller, G. E. & Bleecker, A. B. Ethylene-binding sites generated in yeast expressing the *Arabidopsis* *ETR1* gene. *Science* **270**, 1809–1811 (1995).
10. Maeda, T., Wurgler-Murphy, S. M. & Saito, H. A two-component system that regulates an osmosensing MAP kinase cascade in yeast. *Nature* **19**, 242–245 (1994).
11. Cary, A. J., Liu, W. & Howell, S. H. Cytokinin action is coupled to ethylene in its effects on the inhibition of root and hypocotyl elongation in *Arabidopsis thaliana* seedlings. *Plant Physiol.* **107**, 1075–1082 (1995).
12. Bleecker, A. B., Estelle, M. A. & Somerville, C. Insensitivity to ethylene conferred by a dominant mutation in *Arabidopsis thaliana*. *Science* **241**, 1086–1089 (1988).
13. Lincoln, C., Britton, J. H. & Estelle, M. Growth and development of the *axr1* mutants of *Arabidopsis*. *Plant Cell* **2**, 1071–1080 (1990).
14. Koornneef, M., Reuling, G. & Karssen, C. M. The isolation and characterization of abscisic acid-insensitive mutants of *Arabidopsis thaliana*. *Physiol. Plantarum* **61**, 377–383 (1984).
15. Mähönen, A. P. *et al.* A novel two-component hybrid molecule regulates vascular morphogenesis of the *Arabidopsis* root. *Genes Dev.* **14**, 2938–2943 (2000).
16. Ueguchi, C., Koizumi, H., Suzuki, T. & Mizuno, T. Novel family of sensor histidine kinase genes in *Arabidopsis thaliana*. *Plant Cell Physiol.* (in the press).
17. Posas, F. *et al.* Yeast HOG1 MAP kinase cascade is regulated by a multistep phosphorelay mechanism in the SLN1-YPD1-SSK1 “two-component” osmosensor. *Cell* **86**, 865–875 (1996).
18. Schmitz, R. Y., Skoog, F., Playtis, A. J. & Leonard, N. J. Cytokinins: Synthesis and biological activity of geometric and position isomers of zeatin. *Plant Physiol.* **50**, 702–705 (1972).
19. Urao, T. *et al.* A transmembrane hybrid-type histidine kinase in *Arabidopsis* functions as an osmosensor. *Plant Cell* **11**, 1743–1754 (1999).
20. Miyata, S., Urao, T., Yamaguchi-Shinozaki, K. & Shinozaki, K. Characterization of genes for two-component phosphorelay mediators with a single HPT domain in *Arabidopsis thaliana*. *FEBS Lett.* **437**, 11–14 (1998).
21. Suzuki, T., Imamura, A., Ueguchi, C. & Mizuno, T. Histidine-containing phosphotransfer (HPT) signal transducers implicated in His-to-Asp phosphorelay in *Arabidopsis*. *Plant Cell Physiol.* **39**, 1258–1268 (1998).
22. Kubo, M. & Kakimoto, T. The *CYTOKININ-HYPERSENSITIVE* genes of *Arabidopsis* negatively regulate the cytokinin-signaling pathway for cell division and chloroplast development. *Plant J.* **23**, 385–394 (2000).
23. Becker, D., Kemper, E., Schell, J. & Masterson, R. New binary vectors with selectable markers located proximal to the left T-DNA border. *Plant Mol. Biol.* **20**, 1195–1197 (1992).
24. Akama, K. *et al.* Efficient transformation of *Arabidopsis thaliana*: comparison of the efficiencies with various organs, plant ecotypes and *Agrobacterium* strains. *Plant Cell Rep.* **12**, 7–11 (1992).
25. McKinney, E. C. *et al.* Sequence-based identification of T-DNA insertion mutations in *Arabidopsis*: actin mutants *act2-1* and *act4-1*. *Plant J.* **8**, 613–622 (1995).
26. Hayashi, H., Czaja, I., Lubenow, H., Schell, J. & Walden, R. Activation of a plant gene by T-DNA tagging: auxin-independent growth in vitro. *Science* **258**, 1350–1353 (1992).
27. Mumberg, D., Müller, R. & Funk, M. Yeast vectors for the controlled expression of heterologous proteins in different genetic backgrounds. *Gene* **156**, 119–122 (1995).

Supplementary information is available on Nature's World-Wide Web site (<http://www.nature.com>) or as paper copy from the London editorial office of Nature.

Acknowledgements

M. Higuchi carried out most of the yeast work. We thank H. Saito for yeast strains,

E. Kemper for pGPTV-KAN and K. Torii for comments. Seeds of *abi3-1*, *aux1-7* and *ein2-1* were obtained from ABRC. p415CYC was obtained from ATCC. This study was in part supported by grants from the Ministry of Education, Science and Culture of Japan, and from the Science and Technology Agency to T.K.

Correspondence and requests for materials should be addressed to T.K. (e-mail: kakimoto@bio.sci.osaka-u.ac.jp). The accession numbers for CRE1a and CRE1b are AB049934 and AB049935, respectively.

.....
***cdc2* links the *Drosophila* cell cycle and asymmetric division machineries**

Murni Tio, Gerald Udolph*, Xiaohang Yang and William Chia

Institute of Molecular and Cell Biology, 30 Medical Drive, 117609 Singapore

.....
 Asymmetric cell divisions can be mediated by the preferential segregation of cell-fate determinants into one of two sibling daughters. In *Drosophila* neural progenitors, Inscuteable^{1–3}, Partner of Inscuteable^{4,5} and Bazooka^{6,7} localize as an apical cortical complex at interphase, which directs the apical-basal orientation of the mitotic spindle as well as the basal/cortical localization of the cell-fate determinants Numb^{8,9} and/or Prospero^{10,11} during mitosis. Although localization of these proteins shows dependence on the cell cycle, the involvement of cell-cycle components in asymmetric divisions has not been demonstrated. Here we show that neural progenitor asymmetric divisions require the cell-cycle regulator *cdc2*. By attenuating *Drosophila cdc2* function without blocking mitosis, normally asymmetric progenitor divisions become defective, failing to correctly localize asymmetric components during mitosis and/or to resolve distinct sibling fates. *cdc2* is not necessary for initiating apical complex formation during interphase; however, maintaining the asymmetric localization of the apical components during mitosis requires Cdc2/B-type cyclin complexes. Our findings link *cdc2* with asymmetric divisions, and explain why the asymmetric localization of molecules like Inscuteable show cell-cycle dependence.

The embryonic central nervous system (CNS) of *Drosophila* is derived from progenitors called neuroblasts (NBs). NBs undergo repeated asymmetric divisions, budding off a series of ganglion mother cells (GMCs) from their basal/lateral surfaces; GMCs can divide asymmetrically to produce progeny with distinct neuronal fates. Both the NB and GMC asymmetric divisions are mediated, in part, by a protein localization machinery that directs the preferential segregation of Prospero (Pros) or Numb to the more basally located daughter. Mitosis is driven by activation of the Cdc2 protein kinase, which, during the first 13 embryonic divisions, depends on dephosphorylation by the product of maternal *string* (*cdc25*)^{12,13}. NB divisions occur after depletion of maternal *string* and depend on zygotic *string*. However, NBs, although arrested at G2 of cycle 14, do form in embryos lacking zygotic *string*. In contrast, loss of zygotic *cdc2* does not substantially affect embryonic development, and lethality occurs during postembryonic development^{14,15}.

From a mutant screen we identified two lines that exhibited defective localization of Pros and Inscuteable (Insc) in NBs. Genetic mapping, complementation and DNA sequencing revealed that the phenotypes associated with both mutants were caused by the same mutation in *cdc2*, resulting in a glutamic acid to glutamine change at amino-acid 51. Embryos homozygous for *cdc2*^{E51Q} show late

* Present address: MRC Centre for Developmental Neurobiology, King's College London, London SE1 1UL, UK.

embryonic lethality and exhibit various abnormalities that are also seen in *insc* and *partner of inscuteable (pins)* mutants, which can be explained by defects in asymmetric divisions.

To illustrate these defects, we focused on the first GMC produced from NB4-2, GMC4-2a, which divides to generate two daughter neurons, RP2 and its sibling RP2sib¹⁶. The Even-skipped (*Eve*) protein is expressed in the GMC4-2a sublineages (Fig. 1a). *Eve* is initially expressed in both RP2 and RP2sib; however, its expression is extinguished in RP2sib, such that late in embryonic development only one *Eve*⁺ neuron can be seen at the RP2 position in each wild-type hemineuromere. Two types of defects are seen in *cdc2*^{E51Q} homozygotes. Fourteen per cent of the mutant hemisegments exhibit near the RP2 position a single *Eve*⁺ cell that has all of the characteristics of the RP2 neuron but is larger than the wild-type RP2 neuron. In cell-division mutants that prevent GMC4-2a division, GMC4-2a differentiates into an RP2-like cell that is larger than normal^{17,18} (Fig. 1b; Table 1). More notably, 33% of the mutant hemisegments possess two cells near the RP2 position, both of which show characteristics of the RP2 neuron as judged by marker expression (Fig. 1b, d; Table 1).

Duplication of the RP2 neuron is caused by an RP2sib → RP2 transformation, indicating that the normally asymmetric division of GMC4-2a (GMC4-2a → RP2 + RP2sib), has been converted to a symmetric division (GMC4-2a → RP2 + RP2) in the mutant. This defect in asymmetric division is not restricted to the CNS; the normally asymmetric division of muscle progenitor, P15, which in wild type produces a single *Eve*-expressing muscle DA1 and a second daughter of unknown fate (Fig. 1e), can also become symmetric in mutant embryos, leading to the duplication of muscle DA1¹⁹ (Fig. 1f).

We assessed the localization of *Insc*, *Partner of Numb*²⁰ (*Pon*, which colocalizes with *Numb*) and *Miranda*^{21–23} (which colocalizes with *Pros*) in mutant neural progenitors which are clearly under-

going mitosis. Dividing wild-type GMC4-2a always localizes *Insc* as an apical crescent (20/20; Fig. 2a) and *Pon* as a basal crescent (20/20; Fig. 2d). In dividing *cdc2*^{E51Q} GMC4-2a, defective localization of *Insc* (39%; 9/23; Fig. 2b, c) and *Pon* (37%; 7/19; Fig. 2e, f), in the form of cortical distribution or misplaced crescents, and mis-orientation of the mitotic spindle (Fig. 2f) are observed.

These defects are not restricted to GMCs. Mislocalization of *Insc* (25%, *n* = 246; Fig. 2h), *Bazooka* (38%, *n* = 85; data not shown), *Pon* (Fig. 2k) and *Miranda* (data not shown), and defective spindle orientation (Fig. 2n, o) are also seen in mutant mitotic NBs. These data suggest that the underlying cause of the abnormal progenitor divisions may be the failure to localize the apical components during mitosis, and consequently localization of the basal determinants is also defective. Consistent with this notion, the duplicated RP2 neurons show identical nuclear size—a phenotype characteristic of *insc* and *pins* mutants^{4,17}.

Embryonic lethality and defects in asymmetric division are seen in *cdc2*^{E51Q} embryos but embryos totally lacking zygotic *cdc2* function develop essentially normally (Table 1), owing to the maternal contribution of *cdc2*. Several observations indicate that *cdc2*^{E51Q} acts as a maternal effect dominant-negative allele that can antagonize the maternally inherited wild-type *cdc2*. Strong mutant phenotypes are seen in genotypically hemizygous (*cdc2*^{E51Q}/deficiency) embryos only if the *cdc2*^{E51Q} allele is inherited from the (*cdc2*^{E51Q}/CyO) mother, and not if it comes from the father (Table 1, (2)). Moreover an earlier arrest of cell divisions, resulting in a marked increase in the frequency of undivided GMC4-2a cells, is seen by overexpressing *cdc2*^{E51Q} (from a *uas-cdc2*^{E51Q} transgene) (Table 1, (3)).

To show that defects in asymmetric cell divisions and protein localization are not peculiar to *cdc2*^{E51Q}, we used a stock that is homozygous for an amorphic allele, *cdc2*^{B47}, and in addition contains four copies of a transgene carrying a temperature-sensitive

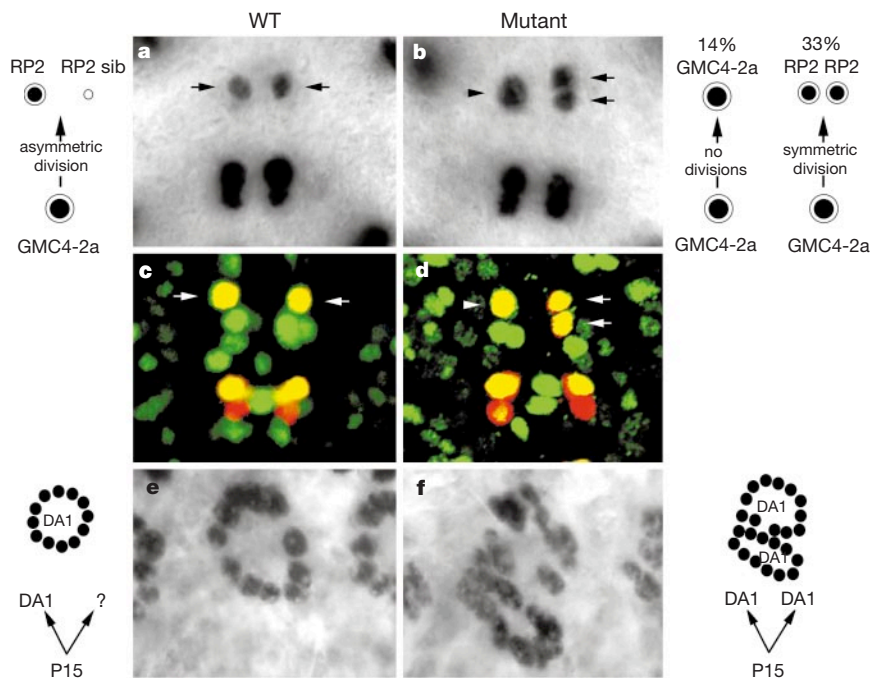


Figure 1 Conversion of asymmetric to symmetric divisions in *cdc2* mutants. **a, b**, Wild-type GMC4-2a divides to produce *Eve*⁺ neurons, RP2 and RP2sib; only RP2 retains *Eve* expression, and by stage 14 only a single *Eve*⁺ neuron can be seen at the RP2 position (arrow, **a**). In *cdc2*^{E51Q} embryos, 14% of GMC4-2a fail to divide and differentiate into a 'large' RP2 (arrowhead, **b**); 33% of GMC4-2a divide symmetrically to give rise to two RP2s with equal nuclear size (arrows, **b**). **c, d**, In addition to *Eve* (red) both wild-type RP2 (**c**) and

the duplicated RP2 and 'large' RP2 found in the mutant (**d**) express *Zfh-1* (green). **e, f**, Muscle progenitor P15 divides to produce one *Eve*⁺ founder for muscle DA1 and a sibling of unknown fate (schematically represented); the single muscle DA1 with about 10 *Eve*⁺ nuclei can be seen from a dorsal–lateral view of a stage 14/15 wild-type embryo (**e**). In *cdc2*^{E51Q} (not shown) or *cdc2ts4X* embryos upshifted to the non-permissive temperature, duplication of the DA1 muscle can be seen (**f**).

allele, *cdc2*^{A171T}, of *cdc2* (referred to as *cdc2ts4X*)²⁴. Immunoprecipitates from *cdc2ts4X* embryonic extracts exhibit kinase activity that is highly temperature sensitive²⁴. Under appropriate temperature-shift conditions, these embryos can exhibit all of the phenotypes seen in *cdc2*^{E51Q} including RP2 (Table 1, (1)) and muscle DA1 (Fig. 1f) duplications, and defective protein localization in dividing progenitors (Fig. 2i, l; and data not shown).

These results suggest that the levels of Cdc2 activity determine whether and how a progenitor divides. When the level of Cdc2 is low, neural progenitors fail to divide; at intermediate levels they can divide, but mitotic NBs often fail to correctly localize asymmetric components, and GMC divisions can become symmetric with respect to segregation of cell-fate determinants and the size and fate of their daughters; only at higher levels of *cdc2* do normal asymmetric divisions take place.

We used a binary expression system²⁵ to express wild-type and mutated forms of *cdc2* in the neural progenitors of *cdc2*^{E51Q} embryos. Expression of a wild-type *cdc2* transgene rescued the *cdc2*^{E51Q} phenotypes, whereas the expression of enzymatically dead versions²⁶ of *cdc2*, *cdc*^{T161A} and *cdc*^{K33R/T161A}, which do not exhibit dominant-negative properties, did not rescue those phenotypes (Table 1, (4)), suggesting that kinase activity is required for

asymmetric divisions. As Cdc2 kinase activity appears to be required to maintain apical Insc localization during mitosis, might it also be required for the apical localization of Insc during interphase? In embryos lacking zygotic *string*, NBs form but arrest at G2 during interphase of cell-cycle stage 14 and fail to enter mitosis because mitotic kinase activation does not occur. Insc (Fig. 3a), Pins and Bazooka (data not shown) form normal apical crescents, indicating that the initial apical localization of the apical components during interphase does not require mitotic kinase activation. Moreover, temperature upshifts can induce similar *string*-like phenotypes in *cdc2ts4X* embryos, and in these embryos the NBs arrested at G2 show apical localization of the apical components (Fig. 3b; and data not shown). These data suggest that Cdc2 kinase activity is required to maintain the apical complex proteins during

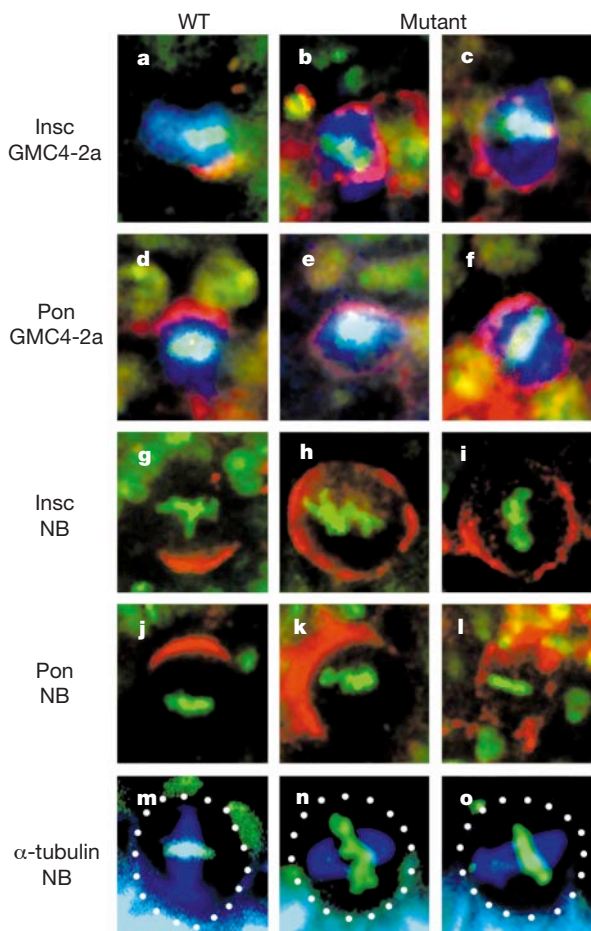


Figure 2 Defective protein localization in dividing neural progenitors of *cdc2* mutants. Lateral optical sections of stage10/11 embryos. Apical is down. **a–c**, Wild-type (**a**) and *cdc2*^{E51Q} (**b, c**) mitotic GMC4-2a labelled with anti-Eve (blue), DNA stain (green) and anti-Insc (red). **d–f**, Wild-type (**d**) and *cdc2*^{E51Q} (**e, f**) mitotic GMC4-2a labelled with anti-Eve (blue), DNA stain (green) and anti-Pon (red). **g–i**, Wild-type (**g, j**), *cdc2*^{E51Q} (**h, k**) and *cdc2ts4X* (**i, l**) mitotic NBs labelled with DNA stain (green) and anti-Insc (red, **g–i**) or anti-Pon (red, **j–l**). **m–o**, Wild-type (**m**) and *cdc2*^{E51Q} (**n, o**) mitotic NBs labelled with DNA stain (green) and anti- α -tubulin (blue). Note the mislocalization of Insc and Pon and the misorientation of mitotic spindles in mutant GMCs and NBs.

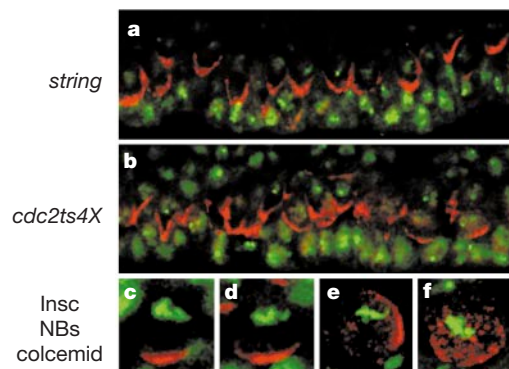


Figure 3 Cdc2 kinase activity is required for the maintenance but not the establishment of Insc apical localization. A *string* embryo arrested at interphase of cycle14 (**a**) and a *cdc2ts4X* embryo shifted to the non-permissive temperature arrested at interphase of cycle 14 (**b**) stained with anti-Insc (red) and DNA stain (green). Note the apical Insc localization in the NBs of both embryos. **c–f**, Wild-type NB treated with colcemid and shifted to 31 °C (**c**); *cdc2ts4X* NB treated with colcemid and maintained at 21 °C (**d**); *cdc2ts4X* NB treated with colcemid and shifted to 31 °C (**e, f**). Insc (red) and DNA (green). Apical is down.

Table 1 Phenotypic analysis of various *cdc2* mutations and genotypes

	RP2 duplication	Big RP2s	n	Lethal phase
Wild type	0%	0%	200	
<i>cdc2</i> ^{E51Q} (amorph)	33%	14%	266	Embryonic
<i>cdc2</i> ^{D57} (amorph)	0.8%	0.8%	381	Larval/pupal
<i>cdc2</i> ^{E1-23} (amorph)	0.25%	0.8%	390	Larval/pupal
<i>cdc2</i> ^{B47} (amorph)	3.6%	3%	307	Larval/pupal
(1) <i>cdc2ts4X</i> *	42.7%	4.6%	144	
(2) <i>cdc2</i> ^{E51Q} / <i>Df(2L)J3</i> from <i>cdc2</i> ^{E51Q} / <i>Cyo(ftz-lacZ)</i> mothers	33%	7%	249	
(2) <i>cdc2</i> ^{E51Q} / <i>Df(2L)J3</i> from <i>cdc2</i> ^{E51Q} / <i>Cyo(ftz-lacZ)</i> fathers	2%	1%	565	
(3) <i>cdc2</i> ^{E51Q} <i>sca-Gal4(1X)</i> ; <i>uas-cdc2</i> ^{E51Q} (1X)	15%	52%	690	
(4) <i>cdc2</i> ^{E51Q} <i>uas-wt cdc2(1X)</i> ; <i>da-Gal4(1X)</i>	0%	0%	486	
(4) <i>cdc2</i> ^{E51Q} <i>uas-T161A(1X)</i> ; <i>da-Gal4(1X)</i>	25.5%	10.5%	475	
(4) <i>cdc2</i> ^{E51Q} <i>uas-K33R, T161A(1X)</i> ; <i>da-Gal4(1X)</i>	22.4%	12%	759	

n is the number of hemisegments scored. The *cdc2* alleles specified represent homozygotes unless otherwise indicated. (1) A viable, fertile stock referred to as *cdc2ts4X*²⁴ (see text). (2) Genotypically *cdc2*^{E51Q}/*Df(2L)J3* embryos show different phenotypes depending on whether the *cdc2*^{E51Q} allele is maternally or paternally inherited. (3) Overexpression of a *cdc2*^{E51Q} transgene using a pan-neural driver, *sca-Gal4*, has dominant-negative effects, increasing the proportion of GMC4-2a which fails to divide. (4) Experiments in which wild-type and enzymatically compromised *cdc2* transgenes were overexpressed in a *cdc2*^{E51Q} homozygous background (using a ubiquitous driver, *da-Gal4*), showing the requirement of kinase activity in asymmetric cell-fate specification. The T161A and the K33R mutations would be expected to compromise cyclin binding and ATP hydrolysis, respectively. Mutant *cdc2* genes were generated by PCR and authenticated by DNA sequencing; germline transformants were produced using standard methods. Temperature shifts were performed as described in Methods.

* The frequency of RP2 duplications is extremely variable in upshifted *cdc2ts4X* embryos and our quantitation was based on ten embryos with the highest frequency of duplications. This phenotype was never seen in wild-type embryos processed in parallel.

mitosis but not for their establishment during interphase.

If Cdc2 activity is responsible for maintaining the apical components, premature inactivation/reduction of its activity—at a point in mitosis when its activity is normally high—should lead to premature delocalization of apical components like Insc. *cdc2ts4X* and wild-type control embryos were arrested at metaphase using colcemid treatment at 21 °C for 30 min (see Methods); half of the embryos were shifted to 31 °C for 45 min, while the other half were kept at 21 °C for 45 min, then both groups were fixed and stained for Insc. *cdc2ts4X* NBs arrested at metaphase and maintained at 21 °C showed normal apical crescents of Insc (98%, $n = 270$; Fig. 3d); similarly, colcemid-treated wild-type controls that were shifted to 31 °C show 100% apical localization ($n = 106$; Fig. 3c). *cdc2ts4X* NBs arrested at metaphase and upshifted to 31 °C showed defective localization of Insc (only 7% have normal apical crescents; $n = 82$; Fig. 3e, f) and Miranda (data not shown). These results show that downregulating Cdc2 activity in NBs

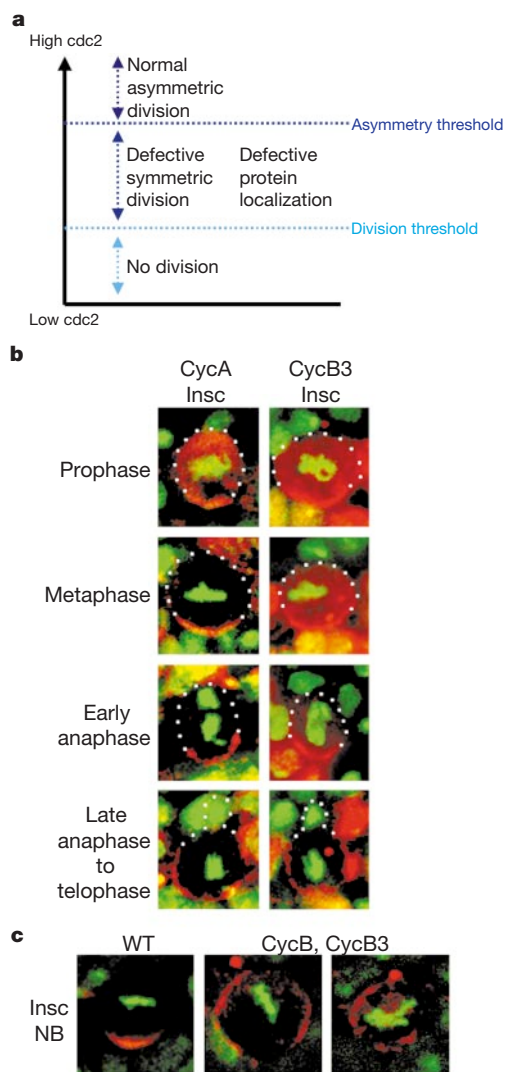


Figure 4 Cdc2 kinase activity is required for asymmetric cell divisions. **a**, Model proposing that different thresholds of kinase activity determine whether and how a progenitor divides (see text). **b**, Wild-type mitotic NBs are stained with anti-Insc (red, apical/cortical), DNA-stain (green) and anti-cyclin-A or anti-cyclin-B3 (red, cytoplasmic). Note that Insc remains localized at metaphase and early anaphase when cyclin A cannot be detected but cyclin B3 levels remain significant. When Insc becomes delocalized (expanded) at late anaphase/telophase, cyclin B3 cannot be detected. **c**, Wild-type metaphase NB (left) and cyclin B, cyclin B3 double-mutant metaphase (middle) and prophase (right) NBs; note the premature delocalization of Insc (red) in the double-mutant NBs.

arrested at metaphase can cause delocalization of the apical (and basal) component proteins and provide direct evidence that elevated Cdc2 activity is required to maintain the localization of apical components during mitosis.

There are three known mitotic cyclins in *Drosophila*, cyclin A, B and B3; these need to be destroyed for mitotic exit to occur²⁷. Is a subset of these cyclins preferentially required for maintaining the apical components? We followed the temporal profile of Insc localization with respect to the time of cyclin A (metaphase), cyclin B (early anaphase) and cyclin B3 (late anaphase) destruction. The results from anti-Insc/anti-cyclin-A/DNA-stain triple-labelling experiments (Fig. 4b) show that Insc remains apically localized at metaphase/anaphase after destruction of cyclin A. Supporting the idea that cyclin A is dispensable, we failed to detect any evidence of defective Insc localization in cyclin A single and cyclin A, cyclin B3 or cyclin A, cyclin B double mutants (data not shown). In wild-type NBs, Insc delocalization occurs after chromosome separation, coinciding with the time when cyclin B3 becomes undetectable (Fig. 4b). Single mutants in cyclin B and cyclin B3 do not show defects in Insc localization (data not shown); however, in cyclin B, cyclin B3 double mutants, mislocalization of Insc can be seen in most mitotic NBs (72%, $n = 120$ for prophase; 71%, $n = 90$ for metaphase; Fig. 4c). These results indicate that whereas cyclin A appears dispensable, the B-type cyclins are required to maintain asymmetric localization of Insc during mitosis.

Our data show that a key cell-cycle regulator is involved in mediating asymmetric cell divisions. Phosphorylation mediated by Cdc2 is likely to be important in maintaining the correct localization of the apical complex of asymmetry proteins during mitosis; however, Cdc2 probably does not act directly on Insc as the putative Cdc2 phosphorylation sites of Insc can be removed without affecting its function in overexpression paradigms^{28,29}. These observations provide an explanation for the normal temporal profile of the localization of molecules like Insc. As long as there is Cdc2 kinase activity during mitosis, apical/cortical localization of molecules such as Insc is maintained; however, when kinase (and B-type cyclins) is destroyed towards the end of mitosis, the apical components become delocalized. Our findings indicate that the tight temporal correlation of asymmetrically localized components important for mediating asymmetric divisions to the cell cycle may be because the two processes share key regulator(s) like *cdc2*. □

Methods

The initial mutant screen

A collection of ~300 lethal enhancer trap insertions that show β -galactosidase expression in all or subsets of NBs were identified and collected over the past few years. We screened embryos from these insertions lines using confocal microscopy after staining with anti-Insc and anti-Pros. The E51Q allele associated with the two lines showing defective Pros and Insc localization were unconnected with their respective P-element insertions, and most probably originated from a pre-existing mutation in the progenitor chromosome used to generate the enhancer traps.

Flies and embryos

The following *cdc2* alleles were used: *cdc2^{E51Q}*, *cdc2ts4X*, *cdc2^{D57}*, *cdc2^{E1-23}* and *cdc2^{B47}*. The following cyclin alleles were used: *cyclinA^{C8LR1}*, *cyclinB²*, *cyclinB3²*, *cyclinB3³*. *string²/TM3 Ubx-lacZ* was used. All lethal mutant alleles that we used in this study were balanced over balancer chromosomes containing P-element insertions expressing *ftz-lacZ* or *Ubx-lacZ*, and homozygous mutant embryos were identified by the absence of β -galactosidase expression. *cdc2ts4X* was raised at 18 °C, and all other stocks were raised at 25 °C. For the temperature-shift experiments designed to examine neuronal or muscle cell fate changes, *cdc2ts4X* embryos were collected for 5 h and aged for 7 h at 21 °C, shifted to 31 °C for 1 h, and aged at 21 °C overnight until fixation. For the temperature-shift experiments designed to examine protein localization in NBs and GMCs, *cdc2ts4X* embryos were dechorionated and incubated in a 31 °C water bath for 1 h before fixation. Wild-type control embryos were processed in parallel.

Drug treatment

Embryos were permeabilized in octane¹² and treated with 20 μ g ml⁻¹ colcemid for 30 min

at 21 °C. They were either maintained at 21 °C or upshifted to 31 °C for a further 45 min before fixation and staining.

Immunohistochemistry

We performed fixation and antibody staining of embryos as described^{4,28}. We used the following primary antibodies: mouse anti- α -tubulin, mouse anti-cyclin-A, mouse anti-cyclin-B, rabbit anti-cyclin-B3, rabbit and mouse anti-Eve, mouse anti-Zfh-1, rabbit and mouse anti- β -galactosidase, rabbit anti-*InsC*, rabbit anti-Miranda, rabbit anti-Pon, mouse anti-Pros. DNA was visualized with a DNA fluorochrome³⁰. Confocal microscopy was performed using a MRC1024 scanhead.

Received 1 November; accepted 7 December 2000.

1. Kraut, R. & Campos-Ortega, J. A. *inscuteable*, a neural precursor gene of *Drosophila*, encodes a candidate for a cytoskeleton adaptor protein. *Dev. Biol.* **174**, 65–81 (1996).
2. Kraut, R., Chia, W., Jan, L. Y., Jan, Y. N. & Knoblich, J. A. Role of *inscuteable* in orienting asymmetric cell divisions in *Drosophila*. *Nature* **383**, 50–55 (1996).
3. Li, P., Yang, X., Wasser, M., Cai, Y. & Chia, W. *inscuteable* and *Staufen* mediate asymmetric localization and segregation of *prospero* RNA during *Drosophila* neuroblast cell divisions. *Cell* **90**, 437–447 (1997).
4. Yu, F., Morin, X., Cai, Y., Yang, X. & Chia, W. Analysis of *partner of inscuteable*, a novel player of *Drosophila* asymmetric divisions, reveals two distinct steps in *inscuteable* apical localization. *Cell* **100**, 399–409 (2000).
5. Schaefer, M., Shevchenko, A., Shevchenko, A. & Knoblich, J. A. A protein complex containing *inscuteable* and the G α -binding protein *Pins* orients asymmetric cell divisions in *Drosophila*. *Curr. Biol.* **10**, 353–362 (2000).
6. Wodarz, A., Ramrath, A., Kuchinke, U. & Knust, E. *Bazooka* provides an apical cue for *inscuteable* localization in *Drosophila* neuroblasts. *Nature* **402**, 544–547 (1999).
7. Schober, M., Schaefer, M. & Knoblich, J. *Bazooka* recruits *inscuteable* to orient asymmetric cell divisions in *Drosophila* neuroblasts. *Nature* **402**, 548–551 (1999).
8. Rhyu, M. S., Jan, L. Y. & Jan, Y. N. Asymmetric distribution of *Numb* protein during division of the sensory organ precursor cell confers distinct fates to daughter cells. *Cell* **76**, 477–491 (1994).
9. Knoblich, J. A., Jan, L. Y. & Jan, Y. N. Asymmetric segregation of *Numb* and *Prospero* during cell division. *Nature* **377**, 624–627 (1995).
10. Hirata, J., Nakagoshi, H., Nabeshima, Y. & Matsuzaki, F. Asymmetric segregation of the homeo-domain protein *Prospero* during *Drosophila* development. *Nature* **377**, 627–630 (1995).
11. Spana, E. & Doe, C. Q. The *Prospero* transcription factor is asymmetrically localised to the cell cortex during neuroblast mitosis in *Drosophila*. *Development* **121**, 3187–3195 (1995).
12. Edgar, B. A. & O'Farrell, P. H. The three postblastoderm cell cycles of *Drosophila* embryogenesis are regulated in G2 by *string*. *Cell* **62**, 469–480 (1990).
13. Edgar, B. A., Sprenger, F., Duronio, R. J., Leopold, P. & O'Farrell, P. H. Distinct molecular mechanisms regulate cell cycle timing at successive stages of *Drosophila* embryogenesis. *Genes Dev.* **8**, 440–452 (1994).
14. Clegg, N. J., Whitehead, I. P., Williams, J. A., Spiegelman, G. B. & Grigliatti, T. A. A developmental and molecular analysis of *cdc2* mutations in *Drosophila melanogaster*. *Genome* **36**, 676–685 (1993).
15. Stern, B., Ried, G., Clegg, N. J., Grigliatti, T. A. & Lehner, C. F. Genetic analysis of the *Drosophila cdc2* homolog. *Development* **117**, 219–232 (1993).
16. Doe, C. Q. Molecular markers for identified neuroblasts and ganglion mother cells in the *Drosophila* central nervous system. *Development* **116**, 855–863 (1992).
17. Buescher, M. *et al.* Binary sibling neuronal cell fate decisions in the *Drosophila* embryonic central nervous system are nonstochastic and require *inscuteable*-mediated asymmetry of ganglion mother cells. *Genes Dev.* **12**, 1858–1870 (1998).
18. Lear, B. C., Skeath, J. B. & Patel, N. H. Neural cell fate in *rcal1* and *cycA* mutants: the roles of intrinsic and extrinsic factors in asymmetric division in the *Drosophila* central nervous system. *Mech. Dev.* **88**, 207–219 (1999).
19. Carmena, A., Murugasu-Oei, B., Menon, D., Jimenez, F. & Chia, W. *inscuteable* and *numb* mediate asymmetric muscle progenitor cell divisions during *Drosophila* myogenesis. *Genes Dev.* **12**, 304–315 (1998).
20. Lu, B., Rothenberg, M., Jan, L. Y. & Jan, Y. N. *Partner of Numb* colocalises with *Numb* during mitosis and directs *Numb* asymmetric localisation in *Drosophila* neural and muscle progenitors. *Cell* **95**, 225–235 (1998).
21. Shen, C. P., Jan, L. Y. & Jan, Y. N. *Miranda* is required for the asymmetric localisation of *Prospero* during mitosis in *Drosophila*. *Cell* **90**, 449–458 (1997).
22. Ikeshima-Kataoka, H., Skeath, J. B., Nabeshima, Y., Doe, C. Q. & Matsuzaki, F. *Miranda* directs *Prospero* to a daughter cell during *Drosophila* asymmetric divisions. *Nature* **390**, 625–629 (1997).
23. Schuld, A. *J. et al.* *Miranda* mediates asymmetric protein and RNA localisation in the developing nervous system. *Genes Dev.* **12**, 1847–1857 (1998).
24. Sigrist, S., Ried, G. & Lehner, C. F. *Dmcdc2* kinase is required for both meiotic divisions during *Drosophila* spermatogenesis and is activated by the *Twine/Cdc25* phosphatase. *Mech. Dev.* **53**, 247–260 (1995).
25. Brand, A. H. & Perrimon, N. Targeted gene expression as a means of altering cell fates and generating dominant phenotypes. *Development* **118**, 401–415 (1993).
26. Ducommun, B. *et al.* *cdc2* phosphorylation is required for its interaction with cyclin. *EMBO J.* **10**, 3311–3319 (1991).
27. Sigrist, S., Jacobs, H., Stratmann, R. & Lehner, C. F. Exit from mitosis is regulated by *Drosophila fizza* and the sequential destruction of cyclins A, B and B3. *EMBO J.* **14**, 4827–4838 (1995).
28. Tio, M., Zavortink, M., Yang, X. & Chia, W. A functional analysis of *inscuteable* and its roles during *Drosophila* asymmetric cell divisions. *J. Cell Sci.* **112**, 1541–1551 (1999).
29. Knoblich, J. A., Jan, L. Y. & Jan, Y. N. Deletion analysis of the *Drosophila inscuteable* protein reveals domains for cortical localization and asymmetric localization. *Curr. Biol.* **9**, 155–158 (1999).
30. Lundell, M. J. & Hirsh, J. A new visible light DNA fluorochrome for confocal microscopy. *Biotechniques* **16**, 434–440 (1994).

Acknowledgements

We thank C. Q. Doe, M. Frasch, D. Glover, M. Harrington, Y.-N. Jan, E. Knust, Z. Lai, K. Matthews, F. Matsuzaki, P. O'Farrell, R. Saint, K. Zinn, the Developmental Studies Hybridoma Bank, Bloomington and Umea Stock Centres, and C. Lehner in particular for stocks and antibodies; F. S. Hing and C. T. Ong for technical support; M. Zavortink, U. Surana and members of our laboratory for comments and discussions; and IMCB for financial support. G.U. is supported by the Wellcome Trust.

Correspondence and requests for materials should be addressed to W.C. (e-mail: mcbwchia@imcb.nus.edu.sg).

Opposing effects of Ets and Id proteins on p16^{INK4a} expression during cellular senescence

Naoko Ohtani*, Zoe Zebedee*, Thomas J. G. Huot†, Julie A. Stinson‡, Masataka Sugimoto*§, Yasuhiro Ohashi||, Andrew D. Sharrocks‡, Gordon Peters† & Eiji Hara*¶

* CRC Cell Cycle Group, Paterson Institute for Cancer Research, Christie Hospital NHS Trust, Manchester M20 4BX, UK

† Imperial Cancer Research Fund Laboratories, London WC2A 3PX, UK

‡ School of Biological Sciences, University of Manchester, Manchester M13 9PT, UK

§ Department of Immunology, Juntendo University Medical School, Tokyo 113-8421, Japan

|| Laboratory of Molecular Biology, Nihon Schering K.K., Osaka 532-0004, Japan

¶ Department of Biomolecular Sciences, University of Manchester Institute of Science and Technology (UMIST), Manchester M60 1QD, UK

The p16^{INK4a} cyclin-dependent kinase inhibitor¹ is implicated in replicative senescence, the state of permanent growth arrest provoked by cumulative cell divisions or as a response to constitutive Ras–Raf–MEK signalling in somatic cells^{2–8}. Some contribution to senescence presumably underlies the importance of p16^{INK4a} as a tumour suppressor⁹ but the mechanisms regulating its expression in these different contexts remain unknown. Here we demonstrate a role for the Ets1 and Ets2 transcription factors¹⁰ based on their ability to activate the p16^{INK4a} promoter through an ETS-binding site and their patterns of expression during the lifespan of human diploid fibroblasts. The induction of p16^{INK4a} by Ets2, which is abundant in young human diploid fibroblasts, is potentiated by signalling through the Ras–Raf–MEK kinase cascade and inhibited by a direct interaction with the helix–loop–helix protein Id1 (ref. 11). In senescent cells, where the Ets2 levels and MEK signalling decline, the marked increase in p16^{INK4a} expression is consistent with the reciprocal reduction of Id1 and accumulation of Ets1.

The p16^{INK4a} tumour suppressor protein functions as an inhibitor of Cdk4 and Cdk6, the cyclin-dependent kinases that initiate the phosphorylation of the retinoblastoma protein, pRb^{9,12}. Thus, p16^{INK4a} has the capacity to arrest cells in the G1 phase of the cell cycle and its probable physiological role is in the implementation of an irreversible growth arrest termed replicative senescence. Senescence occurs naturally when cultured cells reach the end of their lifespan^{13,14}, triggered by the inexorable loss of telomeric DNA^{15,16}, but a similar phenotype can be induced when primary cells are challenged by an activated Ras oncogene or its downstream effectors Raf and MEK^{6–8}. In each case the arrest is accompanied by elevated levels of p16^{INK4a} (refs 2–8) and ectopic expression of p16^{INK4a} in young human diploid fibroblasts (HDFs) the senescent phenotype^{8,17}.

To delineate the signalling pathways that regulate p16^{INK4a} expression in these different contexts, we asked whether existing